Contribution from the Department of Chemistry, University of Florence, Florence, Italy, and Department de Recherche Fondamentale, Centre d'Etudes Nucleaires, Grenoble, France

Crystal Structure and Magnetic Properties of a Copper(II) Chloride Nitronyl Nitroxide Complex Containing Six Exchange-Coupled $S = {}^1/_2$ Spins

Andrea Caneschi,† Fabrizio Ferraro,† Dante Gatteschi,*,† Paul Rey,‡ and Roberta Sessoli†

Received August 15, 1989

A compound of formula $CuCl_2(NITpPy)_2$, where NITpPy = 2-(4-pyridyl)-4,4,5,5-tetramethylimidazolinyl-1-oxyl 3-oxide, was synthesized. It crystallizes in the triclinic $P\bar{1}$ space group with $a = 7.301$ (1) Å, $b = 12.693$ (2) Å, $c = 14.984$ (2) Å, $\alpha = 79.79$ (1)°, $\beta = 86.67$ (1)°, $\gamma = 83.92$ (1)°, and $Z = 2$. The structure consists of dinuclear $[CuCl_2(NITpPy)_2]_2$ centrosymmetric units. The copper atoms are square-pyramidally coordinated by two nitrogen atoms of the pyridine rings and three chlorine atoms, two of them bridging the copper ions. The N–O groups of the radicals belonging to different mononuclear units are at a relatively short separation distance. The analysis of the magnetic susceptibility measurements and of the single-crystal EPR spectra at room and liquid-helium temperatures suggests that the six $S = {}^1/_2$ spins are antiferromagnetically coupled and that the interaction between copper and radical through the nitrogen of the pyridine ring dominates. The interaction between radicals is also significantly different from zero, and structural–magnetic correlations, based on the overlap of the magnetic orbitals, were attempted.

Introduction

Compounds in which nitronyl nitroxides, NITR, are bound to metal ions have provided an exceptionally rich set of different spin clusters, ranging from two to infinite in number.[1-6] The simplest clusters comprise one metal ion directly bound to either one or two nitronyl nitroxides, and the study of their magnetic properties provided basic information on the nature of the exchange interaction between metal ions and radicals, which was the basis for the design[7,8] of one-dimensional ferrimagnets that order as three-dimensional ferromagnets below 10 K.[9-11] Between the simple clusters of two or three spins and the infinite arrays, we also synthesized systems containing a finite but large number of spins.[3,4] The quantitative interpretation of the magnetic properties of these compounds is difficult because the number of spins to be taken into consideration is large and the simplifications determined by the translation symmetry of an infinite lattice are not possible. However, much work can be anticipated in this area, both for the theoretical and the practical interest that these compounds have.[12-18]

We are now searching for nitronyl nitroxide ligands that can yield three-dimensional ferro- or ferrimagnetic structures when bound to metal ions, with the aim to increase the magnetic transition temperature dramatically compared to those of the compounds synthesized so far.[9,11] One possibility is that of varying the R group of the NITR molecules, introducing substituents that can potentially bind to metal ions. In this frame we synthesized the radical NITpPy (2-(4-pyridyl)-4,4,5,5-tetramethyl-

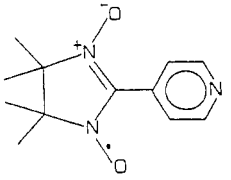

NITpPy

imidazolinyl-1-oxyl 3-oxide), which is potentially tridentate though the pyridine nitrogen and the two oxygen atoms, and we wish to report here the crystal structure of $CuCl_2(NITpPy)_2$, which although has no three-dimensional magnetic character, was found to be formed by dimeric molecules $[CuCl_2(NITpPy)_2]_2$ that allowed us to study the magnetic properties of a cluster of six exchange-coupled $S = {}^1/_2$ spins. The difficulties we found in the interpretation of the magnetic properties are well representative of the difficulties of the systems with large but finite number of spins, and we wish to show the necessity of using more techniques, such as susceptibility measurements and EPR spectroscopy, to obtain meaningful estimations of the exchange interactions. The exchange parameters so obtained allowed us to discuss the mechanism of exchange between metal ions and a nitronyl nitroxide to which they are bound through a peripheral donor atom rather than through an oxygen atom. Furthermore, we discuss the exchange interaction between the N–O groups of the NITR radicals, with the aim to obtain useful structural–magnetic cor-

Table I. Crystallographic Data and Experimental Parameters for $[CuCl_2(NITpPy)_2]_2$

formula	$C_{24}H_{32}N_6O_4Cl_2Cu$	mol wt	603.0
cryst syst	triclinic	space group	$P\bar{1}$
a	7.301 (1) Å	α	79.79 (1)°
b	12.693 (2) Å	β	86.67 (1)°
c	14.984 (2) Å	γ	83.92 (1)°
V	1357.8 Å^3	Z	2
density	1.475 g/cm^3	μ	8.18 cm^{-1}
temp	20 °C	λ	0.7107 Å
refinement	$R = 0.0308$, $R_w = 0.0330$		

(1) Gatteschi, D.; Laugier, J.; Rey, P.; Zanchini, C. *Inorg. Chem.* **1987**, *26*, 938.
(2) Caneschi, A.; Gatteschi, D.; Laugier, J.; Rey, P.; Sessoli, R. *Inorg. Chem.* **1988**, *27*, 1553.
(3) Caneschi, A.; Gatteschi, D.; Hoffmann, S. K.; Laugier, J.; Rey, P.; Sessoli, R. *Inorg. Chem.* **1988**, *27*, 2392.
(4) Caneschi, A.; Gatteschi, D.; Laugier, J.; Rey, P.; Sessoli, R.; Zanchini, C. *J. Am. Chem. Soc.* **1988**, *110*, 2795.
(5) Caneschi, A.; Gatteschi, D.; Laugier, J.; Rey, P. *J. Am. Chem. Soc.* **1987**, *109*, 2191.
(6) Caneschi, A.; Gatteschi, D.; Rey, P.; Sessoli, R. *Inorg. Chem.* **1988**, *27*, 1756.
(7) Caneschi, A.; Gatteschi, D.; Grand, A.; Laugier, J.; Pardi, L.; Rey, P. *Inorg. Chem.* **1988**, *27*, 1031.
(8) Caneschi, A.; Gatteschi, D.; Laugier, J.; Pardi, L.; Rey, P.; Zanchini, C. *Inorg. Chem.* **1988**, *27*, 2027.
(9) Caneschi, A.; Gatteschi, D.; Renard, J. P.; Rey, P.; Sessoli, R. *Inorg. Chem.* **1989**, *28*, 1976.
(10) Caneschi, A.; Gatteschi, D.; Renard, J. P.; Rey, P.; Sessoli, R. *Inorg. Chem.* **1989**, *28*, 2940.
(11) Caneschi, A.; Gatteschi, D.; Renard, J. P.; Rey, P.; Sessoli, R. *Inorg. Chem.* **1989**, *28*, 3314.
(12) Wieghardt, K.; Pohl, K.; Jibril, I.; Huttner, G. *Angew. Chem., Int. Ed. Engl.* **1984**, *23*, 77.
(13) Gorunn, S. M.; Lippard, S. J. *Nature (London)* **1986**, *319*, 666. Gorunn, S. M.; Papaefthymiou, G. C.; Frankel, R. B.; Lippard, S. J. *J. Am. Chem. Soc.* **1987**, *109*, 3337.
(14) Christmas, C.; Vincent, J. B.; Chang, H. R.; Huffman, J. C.; Christou, G.; Hendrickson, D. N. *J. Am. Chem. Soc.* **1988**, *110*, 823.
(15) Boyd, P. D. W.; Li, Q.; Vincent, J. B.; Chang, H. R.; Streib, W. E.; Huffman, J. C.; Christou, G.; Hendrickson, D. N. *J. Am. Chem. Soc.* **1988**, *110*, 8537.
(16) Wieghardt, K.; Bossek, U.; Nuber, B.; Weiss, J.; Bonvoisin, J.; Corbella, M.; Vitols, S. J.; Girerd, J. J. *J. Am. Chem. Soc.* **1988**, *110*, 7398.
(17) Vincent, J. B.; Christmas, C.; Chang, H. R.; Li, Q.; Boyd, P. D. W.; Huffman, J. C.; Hendrickson, D. N.; Christou, G. *J. Am. Chem. Soc.* **1989**, *111*, 2086.
(18) de Jongh, L. J. In *Organic and Inorganic Low Dimensional Crystalline Materials*; Delhaes, P., Drillon, M., Eds.; NATO ASI Series 168; Plenum: New York, 1987.

† University of Florence.
‡ Centre d'Etudes Nucleaires.

0020-1669/90/1329-1756$02.50/0 © 1990 American Chemical Society

Table II. Positional Parameters ($\times 10^4$) and Isotropic Thermal Factors ($Å^2 \times 10^3$) for $[CuCl_2(NITpPy)_2]_2$[a]

	x/a	y/b	z/c	U_{iso}
Cu	816 (1)	917 (1)	4125 (1)	29
Cl1	-2059 (1)	887 (1)	4851 (1)	31
Cl2	3174 (1)	1463 (1)	3140 (1)	51
N1	-2860 (4)	-1851 (3)	940 (2)	40
N2	0 (4)	-1718 (3)	424 (2)	43
N3	22 (4)	54 (2)	3218 (2)	32
N4	2869 (4)	4461 (2)	7103 (2)	37
N5	5521 (4)	4160 (2)	6385 (2)	36
N6	1631 (4)	1798 (2)	5010 (2)	29
O1	-4290 (4)	-1876 (3)	1472 (2)	64
O2	-1625 (4)	-1444 (3)	299 (2)	85
O3	1261 (3)	4338 (3)	7460 (2)	60
O4	6763 (4)	3826 (3)	5849 (2)	71
C1	1317 (5)	-586 (3)	2842 (2)	34
C2	974 (5)	-1134 (3)	2165 (2)	38
C3	-813 (5)	-1046 (3)	1864 (2)	35
C4	-2172 (5)	-426 (3)	2274 (2)	39
C5	-1706 (5)	120 (3)	2937 (2)	37
C6	-1216 (5)	-1546 (3)	1103 (2)	38
C7	-2868 (5)	-2075 (3)	-16 (2)	37
C8	-784 (5)	-2346 (3)	-202 (2)	37
C9	-4072 (7)	-2970 (4)	-51 (3)	66
C10	-3675 (6)	-1036 (3)	-595 (3)	56
C11	-86 (7)	-3514 (3)	129 (3)	56
C12	-85 (6)	-1974 (3)	-1160 (3)	52
C13	3409 (4)	1659 (3)	5228 (2)	33
C14	4152 (4)	2288 (3)	5747 (2)	35
C15	3022 (4)	3100 (3)	6067 (2)	32
C16	1158 (5)	3225 (3)	5869 (3)	39
C17	540 (5)	2560 (3)	5342 (2)	34
C18	3792 (4)	3869 (3)	6529 (2)	33
C19	3899 (5)	5401 (3)	7199 (2)	35
C20	5886 (4)	4928 (3)	6997 (2)	32
C21	3172 (6)	6333 (3)	6486 (3)	55
C22	3532 (6)	5680 (4)	8137 (3)	59
C23	6829 (5)	4236 (3)	7805 (3)	48
C24	7148 (6)	5737 (3)	6498 (3)	50

[a] Standard deviations in the last significant digit are in parentheses.

relations for this type of interaction.

Experimental Section

Synthesis. The radical NITpPy was prepared as previously described.[19] A 1-mmol amount of $CuCl_2 \cdot 2H_2O$ and 2 mmol of NITpPy were separately dissolved in ethanol. The two solutions were allowed to diffuse through a frit. After 2 months green crystals suitable for X-ray analysis were collected. The compound analyzed well for $CuCl_2(NITpPy)_2$. Anal. Calcd for $CuCl_2C_{24}H_{32}N_6O_4$: C, 47.80; H, 5.31; N, 4.65. Found: C, 47.76; H, 5.41; N, 4.55.

X-ray Structure Determination. X-ray data were collected on an Enraf-Nonius CAD4 four-circle diffractometer with Mo Kα radiation at room temperature. Accurate cell parameters were derived by a least-squares refinement of the setting angles of 23 reflections in the range $8° \leq \theta \leq 15°$. Experimental parameters are reported in Table SI of the supplementary material, of which Table I is a condensed form. The data were corrected for Lorentz and polarization effects but not for absorption. The Patterson map revealed the position of the copper atom, while the positions of the other non-hydrogen atoms were found by successive Fourier and difference Fourier syntheses using the SHELX76 package.[20] All non-hydrogen atoms were refined with anisotropic thermal factors, and the final least-squares refinement, including the contribution of hydrogen atoms in idealized position, converged to $R = 0.031$. The highest peak in the last difference Fourier map was less than 0.3 e/Å^3. Atomic positional parameters are listed in Table II, while anisotropic thermal factors and coordinates of hydrogen atoms are available as supplementary material in Tables SII and SIII, respectively.

Magnetic and EPR Measurements. Magnetic susceptibility in the temperature range 5–300 K was measured by using a fully automatized AZTEC DSM5 susceptometer equipped with an Oxford Instruments CF1200S continuous-flow cryostat and a Bruker B-E15 electromagnet. Diamagnetic corrections were estimated from Pascal's constants.

Polycrystalline powder and single-crystal EPR spectra were recorded with a Varian E-9 spectrometer equipped with standard X- and Q-band facilities. Variable-temperature spectra at X-band frequency were recorded by using an Oxford Instruments ESR9 continuous-flow cryostat. A single crystal of $CuCl_2(NITpPy)_2$ was oriented with the diffractometer mentioned above and was found to have the shape of a platelet with largely developed (010) and (0$\bar{1}$0) faces and elongation along the (100) direction.

Calculations. The magnetic susceptibility was fitted by using a minimization procedure based on a standard MINUIT library[21] on a IBM 4361/3 computer. The extended Hückel calculations of the overlap between the π^* magnetic orbitals of two radicals were performed on the same computer with two H_2NO fragments. The H_2NO moieties have C_{2v} symmetry and the following structural parameters: N–O = 1.28 Å, N–H = 1.00 Å, and H–N–O = 120°. The Slater exponents as well as the VSIP parameters are reported in Table SVII (supplementary material).

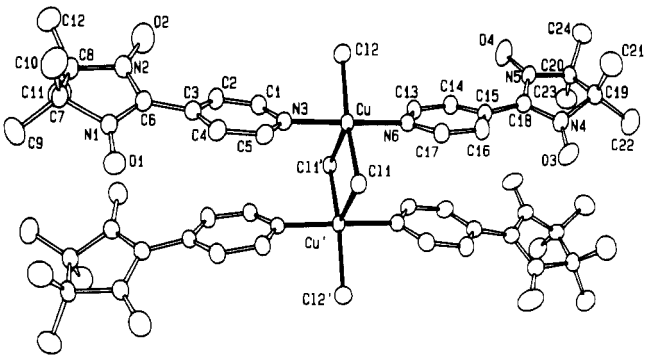

Figure 1. ORTEP view of $[CuCl_2(NITpPy)_2]_2$.

Table III. Selected Bond Distances (Å) and Angles (deg)[a]

Cu–Cl1	2.308 (1)	Cu–Cl1′	2.625 (1)
Cu–Cl2	2.284 (1)	Cu–N3	2.034 (3)
Cu–N6	2.031 (3)	Cu–Cu′	3.431 (1)
O1–N1	1.276 (4)	O2–N2	1.265 (5)
O3–N4	1.274 (3)	O4–N5	1.265 (4)
Cl1–Cu–Cl1′	92.1 (1)	Cl1–Cu–Cl2	160.6 (1)
Cl1–Cu–N3	90.6 (1)	Cl1–Cu–N6	90.2 (1)
Cl1′–Cu–Cl2	107.2 (1)	Cl1′–Cu–N3	89.4 (1)
Cl1′–Cu–N6	91.6 (1)	Cl2–Cu–N3	89.5 (1)
Cl2–Cu–N6	89.5 (1)	N3–Cu–N6	178.9 (1)

[a] Standard deviations in the last significant digit are in parentheses.

Results

Crystal Structure. The structure consists of centrosymmetric $[CuCl_2(NITpPy)_2]_2$ units shown in Figure 1. The copper(II) ions are square-pyramidally coordinated to two chloride ions and to two pyridine nitrogen atoms of two different NITpPy molecules, which occupy equatorial coordination sites, while the axial position is occupied by a chloride ion that belongs to the unit related to the first by the symmetry operation $(-x, -y, 1 - z)$. Selected bond lengths and distances are reported in Table III. The equatorial Cu–Cl bonds are shorter than the axial one (2.284 (1) and 2.308 (1) vs 2.625 (1) Å). The two N–O groups of each NITpPy are practically identical, and the N–O distances are shorter than generally observed[3,4,6,8] in coordinated groups, 1.27 vs 1.29 Å. The carbon atoms carrying the CH_3 groups are not in the plane of the unsaturation. The dihedral angle of this plane with that of the pyridine ring is 31.8° for both radicals. The four radicals, again related by the operation $(-x, -y, 1 - z)$, are stacked in pairs. The N–O groups of two different nitroxides in a pair have the following short contacts: O1–O3 = 3.794 Å, O1–N4 = 3.668 Å, N1–O3 = 3.733 Å, N1–N4 = 4.016 Å. The planes of the stacked pyridines form an angle of 11.9° with each other with an average separation distance of about 3.6 Å.

(19) Ullman, E. F.; Call, L.; Osiecki, J. H. *J. Org. Chem.* **1970**, *35*, 3623. Davis, M. S.; Morokuma, K.; Kreilick, R. W. *J. Am. Chem. Soc.* **1972**, *94*, 5588.

(20) Sheldrick, G. SHELX76 System of Computing Program. University of Cambridge, Cambridge, England, 1976. Atomic scattering factors after: Cromer, D. T.; Liberman, D. J. *J. Chem. Phys.* **1970**, *53*, 1891.

(21) James, F.; Roos, M. *Comput. Phys. Commun.* **1975**, *10*, 343.

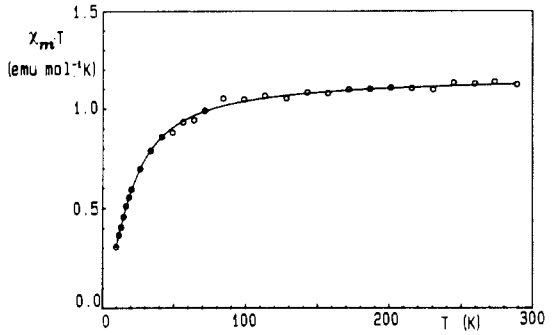

Figure 2. Temperature dependence of $\chi_m T$ for $CuCl_2(NITpPy)_2$. The solid line corresponds to the best fit with $J = 7.4$ cm^{-1}, $J' = 0$ cm^{-1}, $J'' = 19.4$ cm^{-1}, and $g_{Cu} = 2.12$ (see text).

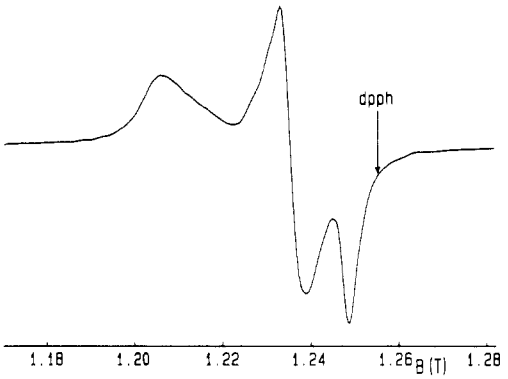

Figure 3. Polycrystalline powder EPR spectrum at room temperature and Q-band frequency.

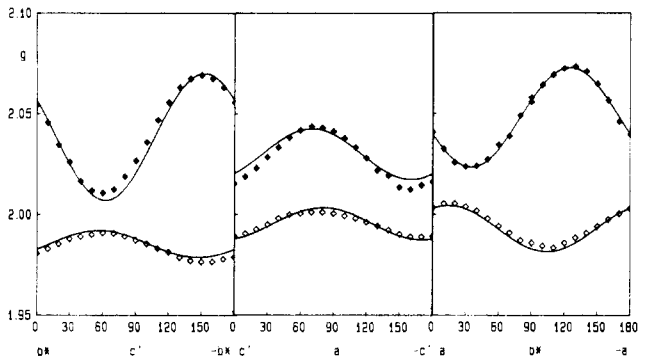

Figure 4. Observed g factors in the rotations along a, b^*, and c at room temperature (◆) and at 4.2 K (◇). The solid lines correspond to the calculated values.

Magnetic and EPR Data. The temperature dependence of χT for $[CuCl_2(NITpPy)_2]_2$ is shown in Figure 2. The room-temperature value of χT, 1.12 emu mol^{-1} K for the monomeric formula, is slightly lower than expected for three uncoupled $S = {}^1/_2$ spins and decreases steadily as the temperature in lowered, showing that the spins are antiferromagnetically coupled. The value at 7 K is 0.21 emu mol^{-1} K, lower than expected for one unpaired electron.

Polycrystalline powder EPR spectra of $[CuCl_2(NITpPy)_2]_2$ recorded at Q-band frequency at room temperature are shown in Figure 3. They are typical of a rhombic $S = {}^1/_2$ spin, with $g_1 = 2.08$, $g_2 = 2.03$, and $g_3 = 2.01$. From the corresponding X-band spectra we could evaluate $g_\parallel = 2.08$ and $g_\perp = 2.03$. At 4.2 K the X-band spectra are clearly rhombic, with principal g values, $g_1 = 2.01$, $g_2 = 1.99$, and $g_3 = 1.98$.

Single-crystal spectra were recorded by rotating around the a, $b^* = a \times c$, and $c' = a \times b^*$ axes at room temperature and at 4.2 K. Only one signal was observed at all crystal orientations in the external magnetic field. The angular dependence of the **g** tensor could be followed with the formulas appropriate to Kramer's doublets.[22] The observed and calculated g values at the two temperatures are shown in Figure 4. The corresponding calculated **g** tensors are given in Table IV. Both polycrystalline powder and single-crystal EPR spectra recorded at intermediate temperatures show that the variation of g values is gradual, and no evidence of any abrupt transition is found. The g values decrease on decreasing temperature, and the direction corresponding to the highest g value at room temperature is close to that of the lowest g value at low temperature as shown in Figure 5. In fact g_1 at room temperature makes an angle of approximately 12° with the Cu–Cl1′ direction, while g_3 at low temperature makes an angle of approximately 10° with the same direction.

Table IV. Principal Values and Directions of the **g** Tensor at Room and Liquid-Helium Temperature[a]

room temp		liq-helium temp	
g	direction	g	direction
$g_1 = 2.08$	0.4860	$g_1 = 2.00$	0.9271
	−0.7866		0.2845
	0.3810		0.2439
$g_2 = 2.03$	−0.8603	$g_2 = 1.99$	0.3518
	−0.3536		−0.4367
	0.3672		−0.8279
$g_3 = 2.01$	0.1541	$g_3 = 1.98$	0.1291
	0.5062		−0.8534
	0.8485		0.5050

[a] The direction cosines of the indicated g_i values are referred to the orthogonal frame ab^*c' defined in the text.

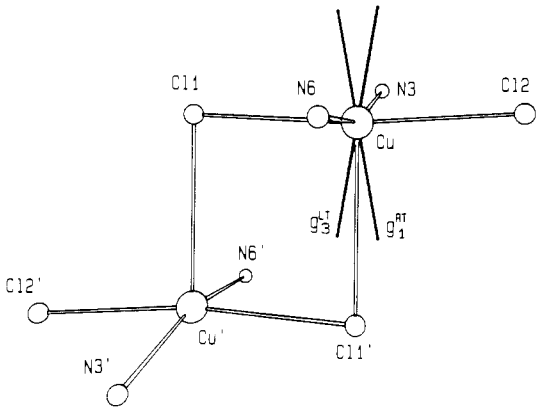

Figure 5. Principal directions of g_1 at room temperature and g_3 at 4.2 K.

Discussion

The simplest scheme of magnetic coupling that we can apply to $[CuCl_2(NITpPy)_2]_2$ is as shown (where 1 and 2 correspond to the spins of the copper):

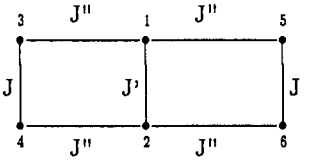

The corresponding spin Hamiltonian is

$$H = J(S_3S_4 + S_5S_6) + J'S_1S_2 + J''(S_1S_3 + S_1S_5 + S_2S_4 + S_2S_6) \quad (1)$$

The energy levels can be obtained for instance by coupling S_1 and S_2 to give S_{12}, S_3 and S_4 to give S_{34}, S_5 and S_6 to give S_{56}, then S_{34} and S_{56} to give S^*, and finally S^* and S_{12} to give S. The energies consequently can be labeled as $E(S_{12}S_{34}S_{56}S^*S)$. There are five $S = 0$, nine $S = 1$, five $S = 2$, and one $S = 3$ states. The $|S_{12}S_{34}S_{56}S^*S\rangle$ basis and the g factors are given in Table V, while the nonzero matrix elements of (1) are given in Table SVI

(22) Schonland, D. S. *Proc. Phys. Soc.* **1959**, *73*, 788.

Table V. Basis Functions $|S_{12}S_{34}S_{56}S^*S\rangle$ and g Factors

no.	basis	g factor	no.	basis	g factor
		$S = 0$			
1	$\|11110\rangle$		4	$\|01100\rangle$	
2	$\|11010\rangle$		5	$\|00000\rangle$	
3	$\|10110\rangle$				
		$S = 1$			
1	$\|11121\rangle$	$g = -{}^1/_2 g_{Cu} + {}^3/_2 g_r$	6	$\|01111\rangle$	$g = g_r$
2	$\|11111\rangle$	$g = {}^1/_2 g_{Cu} + {}^1/_2 g_r$	7	$\|01011\rangle$	$g = g_r$
3	$\|11101\rangle$	$g = g_{Cu}$	8	$\|00111\rangle$	$g = g_r$
4	$\|11011\rangle$	$g = {}^1/_2 g_{Cu} + {}^1/_2 g_r$	9	$\|10001\rangle$	$g = g_{Cu}$
5	$\|10111\rangle$	$g = {}^1/_2 g_{Cu} + {}^1/_2 g_r$			
		$S = 2$			
1	$\|11122\rangle$	$g = {}^1/_6 g_{Cu} + {}^5/_6 g_r$	4	$\|10112\rangle$	$g = {}^1/_2 g_{Cu} + {}^1/_2 g_r$
2	$\|11112\rangle$	$g = {}^1/_2 g_{Cu} + {}^1/_2 g_r$	5	$\|01122\rangle$	$g = g_r$
3	$\|11012\rangle$	$g = {}^1/_2 g_{Cu} + {}^1/_2 g_r$			
		$S = 3$			
1	$\|11123\rangle$	$g = {}^1/_3 g_{Cu} + {}^2/_3 g_r$			

(supplementary material). The magnetic susceptibility can be calculated by using standard procedures[23] allowing for different g values of the different total spin states.

The large number of parameters needed in the fit makes their significant determination rather problematic. The comparison with the structural–magnetic correlation reported for chloride-bridged copper dimers[24] suggests that J' is small ($-8 \leq J' \leq 8$ cm^{-1}). Further sample calculations show that this parameter is the one that least affects the calculated susceptibility. Therefore, we decided to attempt to fit the data by arbitrarily fixing $J' = 0$. The other parameter that can be reasonably fixed is g for copper, which we take as $g_{Cu} = 2.12$, g for the radical being of course $g_r = 2.00$.

The relatively short contacts between radicals 3 and 4 and 5 and 6, respectively, suggest that indeed the exchange constant relative to the radical–radical interaction, J, may be different from zero. The fact that at low temperature the value of the susceptibility is lower than expected for one unpaired electron also requires that J'', the constant relative to the copper–radical interaction, is different from zero. Even with only two parameters, we found that we could obtain satisfactory fits either with $J = 7.4$ cm^{-1}, $J'' = 19.4$ cm^{-1}, and $R = 2.24 \times 10^{-4}$ (fit 1) or with $J = 22.8$ cm^{-1}, $J'' = 12.6$ cm^{-1}, and $R = 2.02 \times 10^{-4}$ (fit 2), where $R = (\sum(y_{cal} - y_{oss})^2/\sum(y_{oss})^2)^{1/2}$. The two solutions are comparable as far as the goodness of fit is concerned; therefore, it is necessary to use additional experimental data to discriminate between them. The EPR spectra do provide such information, because (i) one signal is observed for every crystal orientation, while in principle different signals, with fine structure, would be expected for the different total spin states and (ii) the g values are temperature dependent. A similar behavior was previously observed in trinuclear copper complexes.[25,26] The explanation of this can be that weak intercluster exchange interactions efficiently narrow the lines, averaging the fine structure of all the multiplets. The Lorentzian line shape agrees with this interpretation, which is also justified by the presence of contacts between the N–O groups of the radicals belonging to different molecular units. The temperature dependence of the g values must be determined by the thermal population of the different S states.

At high temperature all the S levels are roughly equally populated, because in these conditions the energy differences are small compared to kT. The g values therefore must correspond to the average of the values of the individual spins, i.e.

$$g = {}^2/_3 g_r + {}^1/_3 g_{Cu} \qquad (2)$$

Using this relation, we predict that the largest g value is observed parallel to the direction of the z molecular axis of the copper center. In fact, we experimentally find that g_1 at room temperature is close to the axial Cu–Cl direction. If we assume $g_r = 2.00$, then (2) yields $g_{Cu1} = 2.24$, which seems to be a reasonable value for a CuN_2Cl_3 chromophore.[27] With the same type of analysis we calculate $g_{Cu2} = 2.09$ and $g_{Cu3} = 2.03$, which again compare well with the value expected for the CuN_2Cl_3 chromophore.[27] The average $g_{Cu} = 2.12$ is the value chosen for the fitting of the susceptibility.

When the temperature decreases, the thermal population of the various S states is varied, and the g values must change, corresponding to a different statistical weight of the various states. The two best fits of the magnetic susceptibility we obtained agree in setting a ground $S = 0$ state, with a triplet at ca. 10 cm^{-1}, which at 4.2 K is thermally populated. The other multiplets are at higher energy and are largely depopulated at 4.2 K. The g values for the different multiplets can be calculated by using the eigenvectors calculated from the diagonalization of the Hamiltonian matrix, and the g values corresponding to the different basis functions are given in Table V. The experimental g values at 4.2 K are smaller than 2, suggesting that in the lowest triplet the $|11121\rangle$ state has a large contribution. In fact, as shown in Table V, this is the only state in which g_{Cu} is present with a negative coefficient. Since $g_{Cu} > g_r$, this yields $g < 2$ for the state. This state corresponds to a dominant J'' interaction, as shown by the expression of the energy, and can be diagrammatically described in the following scheme:

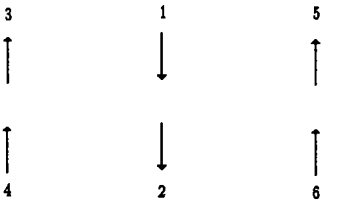

We can expect that for this state the g value parallel to the z molecular axis of the copper center is the smallest, and this is the only one that has this property. Since the experimental **g** tensor at low temperature has in fact the smallest component quasi parallel to the z axis, we conclude that the $|11121\rangle$ state largely contributes to the ground state.

The calculated g values for the low-lying triplets of the two fits of the magnetic susceptibility are largely different from each other. In fact for fit 1, $g = 1.974$, while for fit 2, $g = 2.099$. Therefore, the former appears to be acceptable, indicating that $J = 7.4$ cm^{-1} and $J'' = 19.4$ cm^{-1} better reproduce the experimental data.

The conclusion of the previous analysis is that the copper–radical interaction must be dominant, because only with this scheme we can justify both the magnetic susceptibility and the EPR data. The result can be surprising, because the unpaired electron is essentially localized on the N–O groups and the pyridine nitrogen is rather peripheral. However, ENDOR spectra of the solutions of NITpPy show that a nonzero unpaired spin density is present on the pyridine nitrogen,[28] thus suggesting an effective mechanism for coupling the copper and nitroxide orbitals. The intensity of the interaction is much smaller than that observed in copper nitroxide complexes in which the radical binds in an equatorial position through the oxygen atom, where the coupling constant has been estimated to be larger than 500 cm^{-1}.[1,29–32]

The relatively large coupling constant between copper and NITpPy shows that in principle it might be possible to obtain extended networks of magnetically coupled spins with this radical and appropriate metal ions that can bind to the N–O groups. We are currently working in this direction.

(23) Carlin, R. L. *Magnetochemistry*; Springer-Verlag: New York, 1986.
(24) Hatfield, W. E. In *Magneto-Structural Correlations in Exchange Coupled Systems*; Willett, R. D., Gatteschi, D., Kahn, O., Eds.; NATO ASI Series 140; Reidel: Dordrecht, The Netherlands, 1985.
(25) Banci, L.; Bencini, A.; Gatteschi, D. *Inorg. Chem.* **1983**, *22*, 2681.
(26) Banci, L.; Bencini, A.; Dei, A.; Gatteschi, D. *Inorg. Chem.* **1983**, *22*, 4018.
(27) Bencini, A.; Gatteschi, D. *Transition Met. Chem.* **1982**, *8*, 1.
(28) Ottaviani, F. Private communication.
(29) Lim, Y. Y.; Drago, R. S. *Inorg. Chem.* **1972**, *11*, 1334.
(30) Dickman, M. H.; Doedens, R. J. *Inorg. Chem.* **1981**, *20*, 2671.
(31) Porter, L. C.; Dickman, M. H.; Doedens, R. J. *Inorg. Chem.* **1983**, *22*, 1962.
(32) Porter, L. C.; Doedens, R. J. *Inorg. Chem.* **1985**, *24*, 1006.

Table VI. Geometrical Parameters Relevant to the Exchange Interaction between Noncoordinated NO Groups of Nitronyl Nitroxide Radicals

	r	d	α	β	J_{rr}	ref[34]
$CuCl_2(NITPh)_2$	1.27	3.53	97.9	84	135	33
$[Ni(hfac)_2NITEt]_2$	1.28	3.44	65.3	66	72	2
$[CuCl_2(NITpPy)_2]_2$	1.27	3.73	76.8	56	7.4	this work
		3.67	72.3	79		

Some comments are still in order on the value of the coupling constant between the radicals. We previously determined the values of the coupling constants between NITR radicals in $CuCl_2(NITPh)_2$, $J = 135$ cm^{-1},[33] and $Ni(hfac)_2NITEt$, $J = 72$ cm^{-1}.[2,34] As a consequence, the experimental results show that the coupling between the radicals is in the order $CuCl_2(NITPh)_2 \geq Ni(hfac)_2NITEt \geq CuCl_2(NITpPy)_2$.

In order to try to rationalize the observed trend, we used overlap considerations between the N–O groups in the assumption that the observed coupling constant is the sum of a ferro- and an antiferromagnetic contribution, and the latter is mainly determined by the square of the overlap between the interacting fragments.

The geometrical parameters relevant to the interaction are shown as follows:

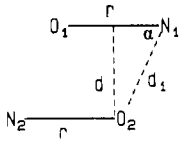

We have made the simplifying assumption that the two groups are related by an inversion center. Beyond the N1–O2 distance, d_1, and the O1–N1–O2 angle, α, the other important parameter is β, the angle between the direction of the π^* orbitals of the NITR radicals and the perpendicular to the plane defined by the N1–O1 and N2–O2 groups. The parameter r is bound to the specific nature of the nitroxide involved in the interaction, and it is also expected to play a role in determining the extent of the magnetic coupling. The values of the parameters for the compounds of interest here are shown in Table VI. We will try to evaluate the role of the parameters that are bound to the reciprocal geometry of the two nitroxides without taking into account the different nature of the individual radicals. Two limit cases can be described, one corresponding to $\beta = 0°$ and the other to $\beta = 90°$. In the former the π^* orbitals of the two fragments overlap in a π fashion, while in the latter the overlap is of the σ type. As a consequence, the antiferromagnetic interaction is expected to be larger for $\beta = 90°$ than for $\beta = 0°$, as shown in Figure 6a.

For a given distance between the two N–O bonds, d, the overlap is maximum for α close to 90° and decreases when α deviates from this value, eventually changing sign. The actual value of the maximum overlap depends on the delocalization of the unpaired electron on the N and O atoms and also on the d_1 distance. Finally, an increase in d_1 will decrease the overlap.

With these considerations in mind we rationalize the observed trend of J values in this way: $CuCl_2(NITPh)_2$ has the highest coupling because it has the β value close to 90°, a relatively short d_1, and α close to 90°. $Ni(hfac)_2NITEt$ is the second because it has a very short d_1, but β and α are rather far from 90°.

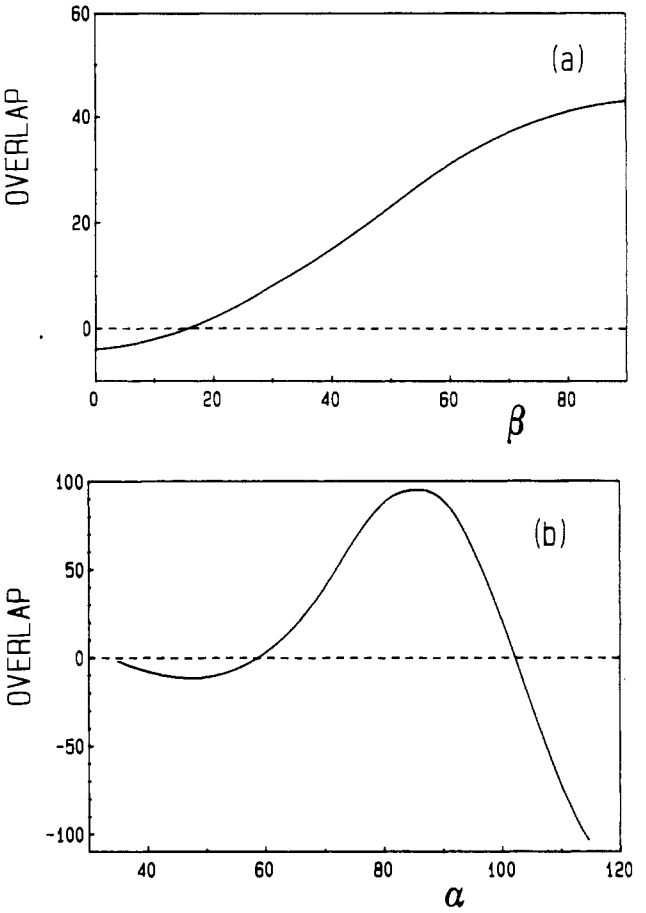

Figure 6. Variation of the overlap (in arbitrary units) between the π^* orbitals of two H_2NO moieties: (a) β varied with $r = 1.28$ Å, $\alpha = 90°$, and $d = 3.0$ Å; (b) α varied with $r = 1.28$ Å, $\beta = 90°$, and $d = 3.0$ Å (see text).

$[CuCl_2(NITpPy)_2]_2$ does not have an inversion symmetry; therefore, the geometrical parameters are rather different one from each other. However, it is apparent that d_1 values are significantly larger than those of the other two compounds and also the β parameters are largely different from 90°. The geometrical parameters seem to justify the small J value shown in Table VI.

Conclusions

The analysis of the magnetic properties of large clusters of spins requires the use of more experimental techniques, and EPR spectroscopy is an ideal tool complementary to magnetic susceptibility measurements.

The most surprising feature of the analysis of the exchange parameters for $[CuCl_2(NITpPy)_2]_2$ is the discovery that the pyridine nitrogen can transmit a significant exchange interaction, opening new exciting perspectives for the use of NITPy ligands in the synthesis of magnetic materials.

Finally, the useful structural–magnetic correlations established here for NITR radicals separated by relatively long distances open new perspectives for understanding long-range interactions between free radicals in crystals.

Acknowledgment. The financial support of the Italian Ministry of Public Education and of the CNR is gratefully acknowledged.

Supplementary Material Available: Table SI, listing experimental and crystallographic parameters, Tables SII and SIII, listing anisotropic thermal parameters and coordinates of hydrogen atoms, Tables SIV and SV, containing bond lengths and angles, Table SVI, listing the nonzero matrix elements in the $|S_{12}S_{34}S_{56}S^*S\rangle$ basis, and Table SVII, listing the parameters of the extended Hückel calculations (9 pages); a table of observed and calculated structure factors (16 pages). Ordering information is given on any current masthead page.

(33) Laugier, J.; Rey, P.; Benelli, C.; Gatteschi, D.; Zanchini, C. *J. Am. Chem. Soc.* **1986**, *108*, 6931.
(34) The values reported in refs 2 and 33 are different, but they are referred to the effective Hamiltonian. The values reported here are relative to the interaction between two radical spins.
(35) Hay, P. J.; Thibeault, J. C.; Hoffmann, R. *J. Am. Chem. Soc.* **1975**, *97*, 4884.
(36) Verdaguer, M.; Michalowitcz, A.; Girerd, J. J.; Alderling, N.; Kahn, O. *Inorg. Chem.* **1980**, *19*, 3271.
(37) Julve, M.; Verdaguer, M.; Kahn, O.; Gleizes, A.; Philoche-Levisalles, M. *Inorg. Chem.* **1983**, *22*, 368.